AGU PUBLICATIONS

Water Resources Research

RESEARCH ARTICLE
10.1002/2014WR016190

Effective parameterizations of three nonwetting phase relative permeability models

Zhenlei Yang[1] and Binayak P. Mohanty[1]

[1]Department of Biological and Agricultural Engineering, Texas A&M University, College Station, Texas, USA

Key Points:
- A generalized nonwetting phase relative permeability expression with Kosugi WRF
- Optimum tortuosity-connectivity parameter for three relative permeability models
- Improved prediction with three modified relative permeability models

Supporting Information:
- Supporting Information S1
- Table S1

Correspondence to:
B. P. Mohanty,
bmohanty@tamu.edu

Citation:
Yang, Z., and B. P. Mohanty (2015), Effective parameterizations of three nonwetting phase relative permeability models, *Water Resour. Res.*, *51*, doi:10.1002/2014WR016190.

Received 24 JUL 2014
Accepted 21 JUL 2015
Accepted article online 27 JUL 2015

Abstract Describing convective nonwetting phase flow in unsaturated porous media requires knowledge of the nonwetting phase relative permeability. This study was conducted to formulate and derive a generalized expression for the nonwetting phase relative permeability via combining with the Kosugi water retention function. This generalized formulation is then used to flexibly investigate the Burdine, Mualem, and Alexander and Skaggs models' prediction accuracy for relative nonwetting phase permeability. The model and data comparison results show that these three permeability models, if used in their original form, but applied to the nonwetting phase, could not predict the experimental data well. The optimum pore tortuosity and connectivity value is thus obtained for the improved prediction of relative nonwetting phase permeability. As a result, the effective parameterization of (α, β, η) parameters in the modified Burdine, modified Mualem, and modified Alexander and Skaggs permeability models were found to be (2.5, 2, 1), (2, 1, 2), and (2.5, 1, 1), respectively. These three suggested models display the highest accuracy among the nine relative permeability models investigated in this study. However, the corresponding discontinuous nonwetting phase and the liquid film flow should be accounted for in future for the improved prediction of nonwetting phase relative permeability at very high and very low water saturation range, respectively.

1. Introduction

Knowledge and understanding of the Nonwetting Phase Relative Permeability (NPRP) are important for accurate characterization of nonwetting phase convective transport processes in the subsurface environment, which subsequently has significant implications for investigating the fate, emission, and transport behavior of volatile organic compounds in the underground [*Falta et al*., 1989], for describing oil-water flow in fractured rock reservoir [*Honarpour et al*., 1986] and for studying the gas exchange and transfer at land-atmosphere interface [*Smits et al*., 2012]. In fact, the relative permeability of the nonwetting phase is an indispensable parameter for the numerical simulation of multiphase flow in the unsaturated zone under both isothermal [*Kueper and Frind*, 1991; *Szymkiewicz et al*., 2011] and nonisothermal conditions [*Mosthaf et al*., 2011; *Mohanty and Yang*, 2013].

In a multiphase system of a porous medium, the relative permeability for a given phase is generally described as a function of the corresponding phase saturation [*Fischer et al*., 1997]. Usually in the unsaturated porous media, liquid water and gas designate the wetting phase and nonwetting phase, respectively [*Dury et al*., 1999; *Kuang and Jiao*, 2011]. Therefore, in this study, relative nonwetting phase permeability and relative gas permeability are used interchangeably.

Without accounting for nonwetting phase entrapment or discontinuities, the existing relative gas permeability-saturation constitutive models can be classified into two categories, namely, the empirical and the statistical models [*Demond and Roberts*, 1993; *Dury et al*., 1999; *Kuang and Jiao*, 2011]. The empirical models generally express NPRP as polynomial functions of wetting phase or nonwetting phase saturation [e.g., *Corey*, 1954; *Falta et al*., 1989]. Apart from the phase saturation, this group of models does not require further parameters to predict the NPRP. As such, the empirical models have the limitation of obtaining the same relative gas permeability for a given effective saturation irrespective of the texture or structure of the porous media [*Dury et al*., 1999]. The statistical models, however, employ idealizations of the pore configuration as a bundle of capillary tubes and utilize the Water Retention Function (WRF) to predict the relative gas permeability-saturation relationships. A large variety of expressions have been proposed to describe the WRFs [e.g., *Brooks and Corey*, 1964; *Brutsaert*, 1966; *van Genuchten*, 1980; *Kosugi*, 1996; *Assouline et al*., 1998].

Combining these WRFs with pore bundle models [e.g., *Burdine*, 1953; *Mualem*, 1976; *Alexander and Skaggs*, 1986] will lead to specific NPRP functions [*Chen et al*., 1999; *Dury et al*., 1999]. For instance, *Chen et al*. [1999] presented seven different closed forms of relative gas permeability functions, which are the Brooks and Corey-Burdine (BCB), Brooks and Corey-Mualem (BCM), van Genuchten-Burdine (VGB), van Genuchten-Mualem (VGM), Russo-Mualem (RUM), Brutsaert-Burdine (BRB), and Kosugi-Mualem (KOM) models. Among them, the BCB and VGM models are so far the most commonly used NPRP representations [*Gerhard and Kueper*, 2003].

It is noticed that the existing statistical models are mostly obtained through the combination of earlier WRFs [e.g., *Brooks and Corey*, 1964; *van Genuchten*, 1980] with pore bundle models. The more recent WRFs [e.g., *Kosugi*, 1996; *Assouline et al*., 1998] are less frequently combined with pore bundle models to derive NPRP models, with the exception of KOM model derived by *Chen et al*. [1999]. The *Assouline et al*. [1998] WRF has not been used so far for evaluating relative gas permeability. Although mathematically more complicated, the advantage of adopting WRF of *Kosugi* [1996] is that the parameters of Kosugi model can be directly related to the statistical properties of the pore-size distribution [*Kosugi*, 1999]. Therefore, in this study, we choose the Kosugi WRF given the fact that the lognormal pore-size distribution has been well documented in various studies for both textured [e.g., *Kosugi*, 1994] and structured [e.g., *Seki*, 2007] porous media.

The existing relative gas permeability models are derived mainly based on the similar principles as used for deriving the relative hydraulic conductivity, with the common practice of using identical pore tortuosity-connectivity exponent values for both relative gas and water permeability for prediction purposes [e.g., *Parker et al*., 1987]. *Tuli and Hopmans* [2004] and *Tuli et al*. [2005] conducted a comparative study between the experimental measured data and the relative gas/water permeability model. They concluded that the tortuosity-connectivity parameter for gas and water relative permeability should be different, largely due to the connections of the corresponding fluid phases and separate flow paths in the porous media. However, they did not suggest the optimum tortuosity-connectivity parameter for predictive relative gas permeability models. Although the tortuosity-connectivity parameter for relative hydraulic conductivity was obtained to be 0.5 by *Mualem* [1976], a comparable study could not be found with respect to the NPRP to date [*Dury et al*., 1999].

Motivated by this and other limitations, such as the less use of the recent WRF and lack of model comparison with a wide variety of soil textures' measured data, this study first formulated and derived a generalized expression for the NPRP model by adopting the Kosugi WRF. Then based on the generalized NPRP formulation and its application to the observed data sets having a large diversity in soil texture, we specifically investigated the effective parameterizations of three pore bundle permeability models [i.e., *Burdine*, 1953; *Mualem*, 1976; *Alexander and Skaggs*, 1986] for their improved descriptions of the relative gas permeability. Meanwhile, the optimum tortuosity-connectivity parameter for the NPRP is obtained for the three investigated relative permeability models.

2. Theory

2.1. Water Retention Function

When conceptualizing the porous medium as a bundle of intersecting capillary tubes with a pore radii distribution function, $f(r)$ (L^{-1}), the contribution of water-filled pores of radii $r \rightarrow r + dr$ to the volumetric water content θ ($L^3\ L^{-3}$) can be formulated as $d\theta(r) = f(r)dr$ ($L^{-1}\ L$) [*Mualem*, 1976; *Assouline*, 2001; *Nasta et al*., 2013a]. According to *Kosugi* [1996], the $f(r)$ function based on a lognormal probability distribution is expressed as

$$f(r) = \frac{\theta_s - \theta_r}{r\sigma\sqrt{2\pi}} \exp\left\{-\left[\frac{\ln(r/r_m)}{\sigma\sqrt{2}}\right]^2\right\} \quad (1)$$

where θ_s ($L^3\ L^{-3}$) and θ_r ($L^3\ L^{-3}$) denote the saturated and residual volumetric water content, respectively. $\ln r_m$ and σ are the mean and standard deviation of the natural logarithm of the porous media pore radius r (L), respectively. The soil matric potential head h (L), is associated with the pore radius r (L), through the Young-Laplace capillary pressure function

$$h=\frac{2\gamma\cos\varpi}{r\rho_w g} \tag{2}$$

in which γ is the surface tension between the liquid water and gas (F L^{-1}), ϖ is the contact angle between the solid and liquid water, ρ_w is the density of liquid water (M L^{-3}), and g is the gravitational acceleration (L T^{-2}). Typically, the value of $2\gamma\cos\varpi/\rho_w g$ for gas-water-porous media system is approximately equal to a constant 1.49×10^{-5} m^2 when h and r are expressed in units of meters [*Brutsaert*, 1966].

On the basis of equations (1) and (2), *Kosugi* [1996] derived the following WRF

$$S_e(h)=\frac{\theta-\theta_r}{\theta_s-\theta_r}=\frac{1}{2}erfc\left[\frac{\ln(h/h_m)}{\sigma\sqrt{2}}\right] \tag{3}$$

where S_e represents effective wetting phase saturation that varies from 0 (when $\theta=\theta_r$) to 1 (when $\theta=\theta_s$), *erf c* denotes the complementary error function. Notice that h_m ($h_m=1.49\times10^{-5}/r_m$) represents the median matric potential head (m) for which $S_e(h_m)=0.5$ [*Kosugi*, 1996; *Tuli and Hopmans*, 2004].

2.2. General Expression for NPRP

Combining the Hagen-Poiseuille equation which is valid at the pore scale with the Darcy equation which is valid at the Representative Elementary Volume (continuum) scale, the statistical approach can be employed to derive the wetting phase [e.g., *Mualem and Dagan*, 1978] and nonwetting phase [e.g., *Helmig*, 1997] relative permeabilities. After *Helmig* [1997] and *Kuang and Jiao* [2011], the generalized expression for the NPRP $k_{rn}(S_e)$, can be written as

$$k_{rn}(S_e)=\frac{k_n(S_e)}{k_{sn}}=T(S_e)G(S_e)\left\{\frac{\int_{S_e}^{1}h^{-\beta}dS_e(h)}{\int_{0}^{1}h^{-\beta}dS_e(h)}\right\}^{\eta}=(1-S_e)^{\alpha}\left\{\frac{\int_{S_e}^{1}h^{-\beta}dS_e(h)}{\int_{0}^{1}h^{-\beta}dS_e(h)}\right\}^{\eta} \tag{4}$$

where k_n (L T^{-1}) and k_{sn} (L T^{-1}) are the unsaturated and saturated nonwetting phase permeability [*Tuli and Hopmans*, 2004], respectively. $T(S_e)$ is a tortuosity factor that accounts for flow path eccentricity (departure from ideal straight capillaries), and $G(S_e)$ accounts for connectivity among the gas-conducting pores [*Kuang and Jiao*, 2011; *Nasta et al*., 2013a]. It is worth mentioning that equation (4) neglects the possible presence of a discontinuous nonwetting phase (trapped and locally accessible) in the porous media [*Fischer et al*., 1997; *Dury et al*., 1999], therefore, the NPRP is described as a function of the total nonwetting phase saturation in equation (4) [*Fischer et al*., 1997; *Dury et al*., 1999].

The parameter α in equation (4), originally proposed by *Burdine* [1953] and later adopted by *Mualem* [1976] as well as other researchers [e.g., *Alexander and Skaggs*, 1986; *Luckner et al*., 1989], is related to the pore tortuosity-connectivity of the porous media. The parameter β in equation (4) is associated with the microscopic pore tortuosity [*Fatt and Dykstra*, 1951; *Kosugi*, 1999]. Whereas the parameter η in equation (4) defines the pore configuration and reflects the way to evaluate the effective pore radius [*Raats*, 1992; *Kosugi*, 1999]. The parameters (α,β,η) in equation (4) can be varied to obtain more specific functional expressions. For the *Purcell* [1949] and *Burdine* [1953] models, parameters (α,β,η) are equal to (0, 2, 1) and (2, 2, 1) respectively, for the *Mualem* [1976] and *Alexander and Skaggs* [1986] models, parameters (α,β,η) are specified as (0.5, 1, 2) and (1, 1, 1) respectively, whereas for the *Luckner et al*. [1989] and *Kuang and Jiao* [2011] models, parameters (α,β,η) are equal to (1/3, 1, 2) and (0.5, 1, 4) respectively. In the *Assouline* [2001] model, $\alpha=0$, $\beta=1$, and η is proposed to be linked to the coefficient of variation of the WRF. It should be pointed that the *Purcell* [1949] model and *Mualem* [1976] model were originally developed for the relative water permeability prediction. They were extended for the NPRP evaluation later by *Burdine* [1953], *Parker et al*. [1987], and other researchers, who usually adopted the same α values as those in the corresponding relative water permeability models, which is probably inappropriate [*Dury et al*., 1999; *Tuli and Hopmans*, 2004; *Tuli et al*., 2005].

2.3. Generalized Formulation for NPRP With Kosugi WRF

Inserting equation (3) into equation (4), one can obtain the generalized relative gas permeability model based on the lognormal pore-size distribution (see Appendix A for the derivation)

Table 1. Data Sets Investigated in This Study and Fitted Parameters for the Kosugi Water Retention Function

Reference	Medium Type	Condition	Porosity	θ_s	θ_r	h_m, (m)	σ	RMSE	R^2
Collis-George [1953]	Cambridge sand	Disturbed	0.380	0.380	0.034	0.148	0.136	0.012	0.995
Brooks and Corey [1964]	Volcanic sand	Unconsolidated	0.351	0.351	0.055	0.229	0.272	0.010	0.993
Brooks and Corey [1964]	Glass beads	Unconsolidated	0.370	0.370	0.036	0.323	0.091	0.011	0.994
Brooks and Corey [1964]	Fine sand	Unconsolidated	0.377	0.377	0.066	0.503	0.269	0.007	0.997
Brooks and Corey [1964]	Touchet silt loam	Unconsolidated	0.485	0.485	0.186	1.044	0.272	0.008	0.994
Brooks and Corey [1964]	Fragmented mixture	Unconsolidated	0.443	0.443	0.134	0.226	0.253	0.009	0.995
Brooks and Corey [1964]	Fragmented Fox Hill	Unconsolidated	0.470	0.470	0.156	0.151	0.445	0.007	0.997
Brooks and Corey [1964]	Berea sandstone	Consolidated	0.206	0.206	0.066	0.515	0.269	0.002	0.994
Brooks and Corey [1964]	Hygiene sandstone	Consolidated	0.250	0.250	0.151	0.640	0.193	0.002	0.992
Brooks and Corey [1966]	Poudre river sand	Unconsolidated	0.364	0.364	0.060	0.171	0.263	0.008	0.995
Brooks and Corey [1966]	Amarillo silty clay loam	Unconsolidated	0.455	0.455	0.138	0.512	0.346	0.010	0.993
Touma and Vauclin [1986]	Grenoble sand	Disturbed	0.370	0.310	0.054	0.318	0.782	0.003	0.998
Stonestrom [1987]	Oakley sand	Disturbed	0.365	0.322	0.105	0.459	0.315	0.009	0.989
Dury [1997]	Mixed sand	Disturbed	0.360	0.285	0.021	0.339	0.316	0.006	0.995
Springer et al. [1998]	Silty sand	Disturbed	0.431	0.431	0.026	0.963	1.939	0.014	0.986
Tuli and Hopmans [2004]	Columbia sandy loam	Disturbed	0.466	0.432	0.098	2.068	1.491	0.007	0.996
Tuli and Hopmans [2004]	Oso Flaco fine sand	Disturbed	0.419	0.406	0.072	0.559	0.287	0.014	0.981

$$k_{rn}=(1-S_e)^{\alpha}\left\{1-\frac{1}{2}erfc\left[erfc^{-1}(2S_e)+\frac{\beta\sigma}{\sqrt{2}}\right]\right\}^{\eta} \tag{5}$$

where $erfc^{-1}$ is the inverse complementary error function. It should be noted that equation (5) is an extension of equation (12) in *Kosugi* [1999] which described the generalized relative hydraulic conductivity model. However, to our knowledge, the generalized equation (5) was obtained for the first time in the literature in terms of relative gas permeability, although one specific case of equation (5), i.e., the KOM model, was already derived by *Chen et al*. [1999].

3. Materials and Methods

3.1. Testing Data Sets

Seventeen experimental data sets [*Kuang and Jiao*, 2011; *Ghanbarian-Alavijeh and Hunt*, 2012] are taken from the literature to evaluate the performance of the generalized k_{rn} model expressed by equation (5). These data sets consisted of laboratory measured curves for both soil water retention and relative nonwetting phase permeability. All these 17 porous media samples (15 unconsolidated soils and 2 consolidated sandstones) shown in the Table 1 are under disturbed conditions and thus have unimodal pore system.

The Kosugi WRF was fitted to the observed water retention data pairs $S(h)$. Here S denotes wetting phase (water) saturation and can be transferred to volumetric water content θ (L^3 L^{-3}) through the expression $\theta=\varphi S$, in which φ (L^3 L^{-3}) is the porosity of the media. For each porous medium, the optimized parameters θ_s, θ_r, h_m, and σ in equation (3) were determined using the "lsqcurvefit" function in the MATLAB optimization toolbox (The MathWorks, Inc.). The fitted values are shown in Table 1. From Table 1, one can notice that all 17 porous media samples can be described by the Kosugi WRF reasonably well because the root mean square error (RMSE) is usually small and the coefficient of determination (R^2) of the curve fitting was always greater than 0.98. The σ values of Glass beads and Silty sand are the smallest and the largest, respectively. Figure 1a displays the observed soil water retention data and the respective optimized curves of Glass beads and Silty sand computed from equation (3). Whereas Figure 1b plots the pore-size distribution of these two soil samples calculated based on equation (1).

3.2. Model Test

Similar to *Kosugi* [1999] and *Kuang and Jiao* [2011], the root mean square error (RMSE) between experimental data and model prediction, was chosen as the objective function and calculated for each porous medium sample to evaluate the performance of equation (5).

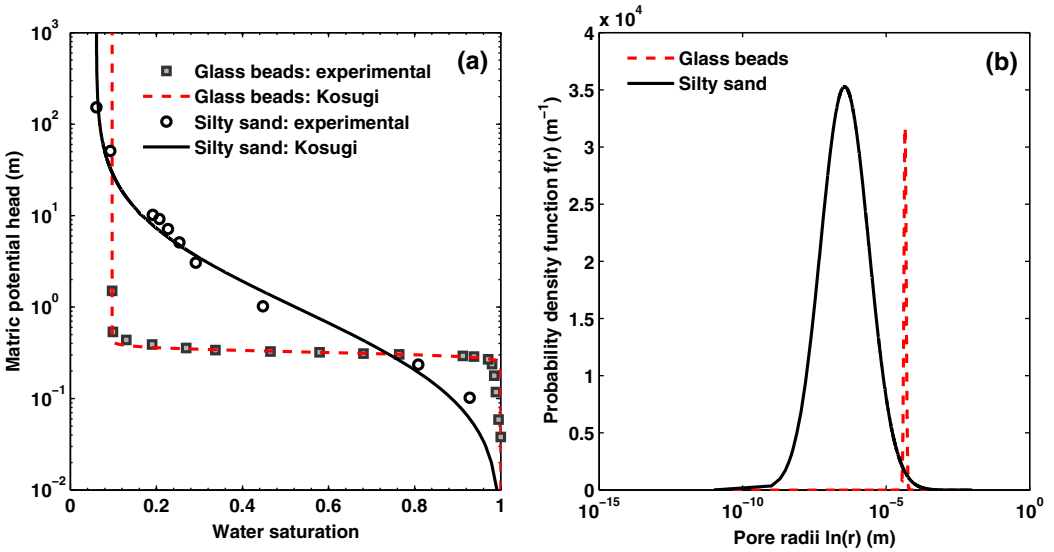

Figure 1. (a) Water retention curves and (b) Pore-size distribution of Glass beads and Silty sand.

$$RMSE = \sqrt{\frac{1}{N-m}\sum_{i=1}^{N}\left[k_{rn,i} - \hat{k}_{rn,i}(S_{ei})\right]^2} \tag{6}$$

where $k_{rn,i}$ and $\hat{k}_{rn,i}(S_{ei})$ are the observed and calculated relative gas permeability, respectively. N is the number of measurements for each experimental sample. m is the number of fitted parameters. The accuracy of equation (5) for the entire data sets was evaluated by employing the average value of the RMSE (aveRMSE) for all the 17 porous media samples [*Kosugi*, 1999; *Kuang and Jiao*, 2011]. For the consistency with previous researchers [*Tuli and Hopmans*, 2004; *Kuang and Jiao*, 2011; *Ghanbarian-Alavijeh and Hunt*, 2012] who used the same data sets to perform the computation and analysis on linear scale, the results obtained on the linear scale are presented below, which are similar to that acquired on the logarithmic scale (supporting information Figures S1–S3).

Equation (5) was tested in its ability to describe the observed nonwetting phase relative permeability data. As Table 2 shows, first, the k_{rn} prediction was tested by using the original coefficients given by the models of Burdine (B), Mualem (M), and Alexander and Skaggs (AS), respectively. Then, 21 other model combinations were created by allowing first one, then two, and eventually all three semiempirical parameters (α, β, and η) to vary [*Kosugi*, 1999; *Hoffmann-Riem et al*., 1999]. These 21 model sets with one, two, or finally three degrees of freedom were fitted to the measured data and compared with respect to the accuracy of the fits. The fitting was conducted via using the "globalsearch" function in the MATLAB global optimization toolbox. With respect to the boundary of the optimized parameter space, both α and β were set to range from -20 to 20 based on the prior knowledge from *Kosugi* [1999], whereas η was set to range from 0.1 to 10 according to the previous experience from *Assouline* [2001] and *Nasta et al*. [2013a, 2013b].

4. Results and Discussions

4.1. Model and Data Comparison

4.1.1. No Fitted Parameter Case

Figures 2, 3, and 4 display the scatter charts of observed versus calculated relative gas permeability based on the model sets B1 to AS8 listed in the Table 2. Figures 2a and 4a show that both B1 and AS1 cases mainly overestimated the measured relative gas permeability values, although they could underestimate the measured data significantly for some relatively fine textured soils. It can be seen in Figure 3a that the M1 case overestimated for all the 17 samples. Notice that the B1, M1, and AS1 cases are identical to the original Burdine, Mualem, and Alexander and Skaggs' predictive models, respectively. The significant deviations from the 1:1 lines for the cases B1, M1, and AS1 indicated some inadequate predictions of k_{rn} values by the

Table 2. Average (aveRMSE), Standard Deviation (stdRMSE), and Maximum (maxRMSE) Values of Root Mean Square Error (RMSE) for the 17 Data Sets by the Cases B1 Through AS8

Cases	α	β	η	aveRMSE	stdRMSE	maxRMSE
B1[a]	2	2	1	0.092	0.066	0.270
B2	Fitted	2	1	0.048	0.039	0.154
B3	2	Fitted	1	0.056	0.065	0.287
B4	2	2	Fitted	0.063	0.067	0.287
B5[b]	Fitted	Fitted	1	0.044	0.037	0.147
B6	Fitted	2	Fitted	0.047	0.043	0.164
B7	2	Fitted	Fitted	0.050	0.071	0.307
B8[c]	Fitted	Fitted	Fitted	0.035	0.029	0.126
M1[a]	0.5	1	2	0.153	0.078	0.330
M2	Fitted	1	2	0.048	0.037	0.141
M3	0.5	Fitted	2	0.047	0.032	0.123
M4	0.5	1	Fitted	0.058	0.049	0.199
M5	Fitted	Fitted	2	0.042	0.034	0.129
M6[d]	Fitted	1	Fitted	0.043	0.033	0.135
M7	0.5	Fitted	Fitted	0.038	0.031	0.118
M8[c]	Fitted	Fitted	Fitted	0.035	0.029	0.126
AS1[a]	1	1	1	0.160	0.060	0.307
AS2	Fitted	1	1	0.048	0.038	0.148
AS3	1	Fitted	1	0.051	0.036	0.148
AS4	1	1	Fitted	0.055	0.042	0.146
AS5[b]	Fitted	Fitted	1	0.044	0.037	0.147
AS6[d]	Fitted	1	Fitted	0.043	0.033	0.135
AS7	1	Fitted	Fitted	0.041	0.039	0.151
AS8[c]	Fitted	Fitted	Fitted	0.035	0.029	0.126

[a]Predictive models.
[b]B5 and AS5 are the identical case from the fitting perspective.
[c]B8, M8, and AS8 are the identical case from the fitting perspective.
[d]M6 and AS6 are the identical case from the fitting perspective.

Burdine, Mualem, and Alexander and Skaggs models. In addition, the average value of RMSE for the whole data sets is the largest for the case AS1, followed by the case M1 and case B1 among the 24 scenarios (Table 2). As such, further improvement is clearly warranted for the improved relative gas permeability description of the original Burdine, Mualem, and Alexander and Skaggs pore bundle models.

4.1.2. Fitted Parameter Case

Figures 2b, 2c, 2d, 3b, 3c, 3d, 4b, 4c, and 4d show that the estimation of k_{rn} values are improved via treating one of the parameters (α, β, and η) as an optimized parameter. Such improvement occurs mainly because the overestimation errors are largely reduced. As a result, the aveRMSE is reduced nearly one order of magnitude compared to that of the original Burdine, Mualem, and Alexander and Skaggs relative permeability models. The reductions in aveRMSE were 48%, 39%, and 31% for the cases B2, B3, and B4, respectively, compared to the case B1, 69%, 70% and 62% for the cases M2, M3 and M4, respectively, compared to the case M1, and 70%, 68%, and 65% for the cases AS2, AS3, and AS4, respectively, compared to the case AS1 (see Table 2). The range of optimized α value is (1.00, 4.49), (0.89, 3.60), and (0.95, 4.25) with the average values 2.73, 1.95, and 2.52 for the cases B2, M2, and AS2, respectively. Whereas the fitted β value is mostly negative. This is reflected by the fact that the averages of optimized β value in B3, M3, and AS3 cases are -0.08, -0.77, and -2.14, respectively. The reductions in aveRMSE were the smallest when treating η as a fitting parameter compared to that of treating either α or β as a fitting parameter.

Figures 2e, 2f, 2g, 3e, 3f, 3g, 4e, 4f, and 4g show that the prediction of k_{rn} values are further improved by treating two of the three parameters as fitted ones. It is worth pointing out that such further improvement is not quite significant compared to the cases using only one fitted parameter. As a matter of fact, the aveRMSE value obtained using two fitted parameters is on the same order of magnitude with that of using one fitted parameter (Table 2).

The prediction of k_{rn} values in cases B8, M8, and AS8 versus measured values is plotted in Figures 2h, 3h, and 4h, which display an excellent linearity around 1:1 lines. It is expected that the B8, M8, and AS8 cases have the smallest aveRMSE since they have the largest degree of freedom of fitted parameters.

4.2. Optimum α Parameter for NPRP

The model and comparison results shown above indicate that the original B, M, and AS pore bundle models lead to the worst predictions of the NPRP, allowing one parameter (either one) to vary can improve the fit significantly, and further increasing the degrees of freedom to two and three yields an even better fit, though with less improvement as compared to the one fitted parameter case. This finding is consistent with *Kuang and Jiao* [2011], who modified the η value in Mualem model from 2 to 4 to arrive at their new NPRP model that increases the predictive ability. However, in this study we attempt to modify the α value in the B, M, and AS relative permeability models as the way to solve the problem that the optimum α values in the three permeability models are largely unknown so far [*Dury et al.*, 1999]. To that end, similar to *Kuang and Jiao* [2011], several discrete values of α which ranged from 0 to 4.5 were adopted in this work. For each

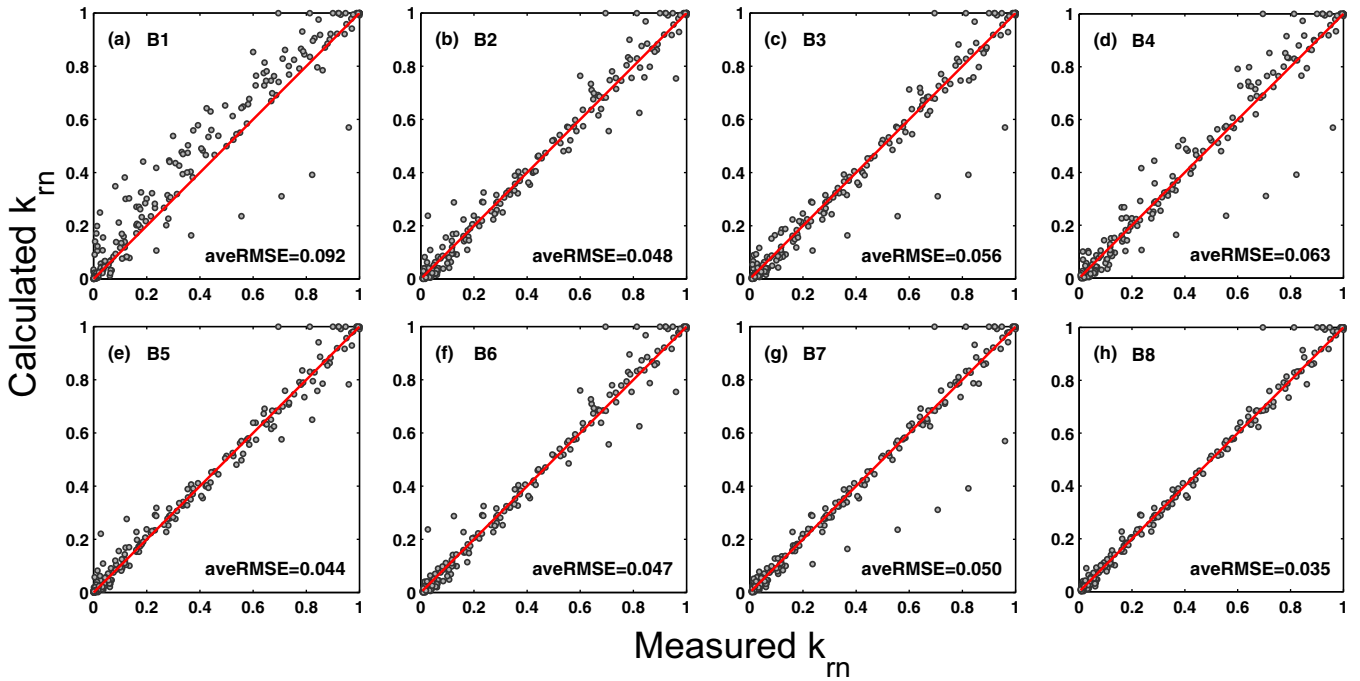

Figure 2. Scatter charts of measured versus calculated relative gas permeability for the cases (a) B1, (b) B2, (c) B3, (d) B4, (e) B5, (f) B6, (g) B7, and (h) B8 for the 17 data sets.

sample and each value of α, the RMSE between model and data was calculated. Then at each discrete α value, the average RMSE was computed for the entire 17 samples. Figures 5a, 5b, and 5c plot the variations of the average RMSE with α for the Burdine, Mualem, and Alexander and Skaggs models, respectively. As a result, the optimum α values for the respective pore bundle models can be obtained. Notice that in Firgure 5a, α=0 corresponds to the *Purcell* [1949] model, which has the largest mean RMSE. This indicated that the pore tortuosity and conectivity effect for calculating k_{rn} value should not be ignored. Firgure 5a displays

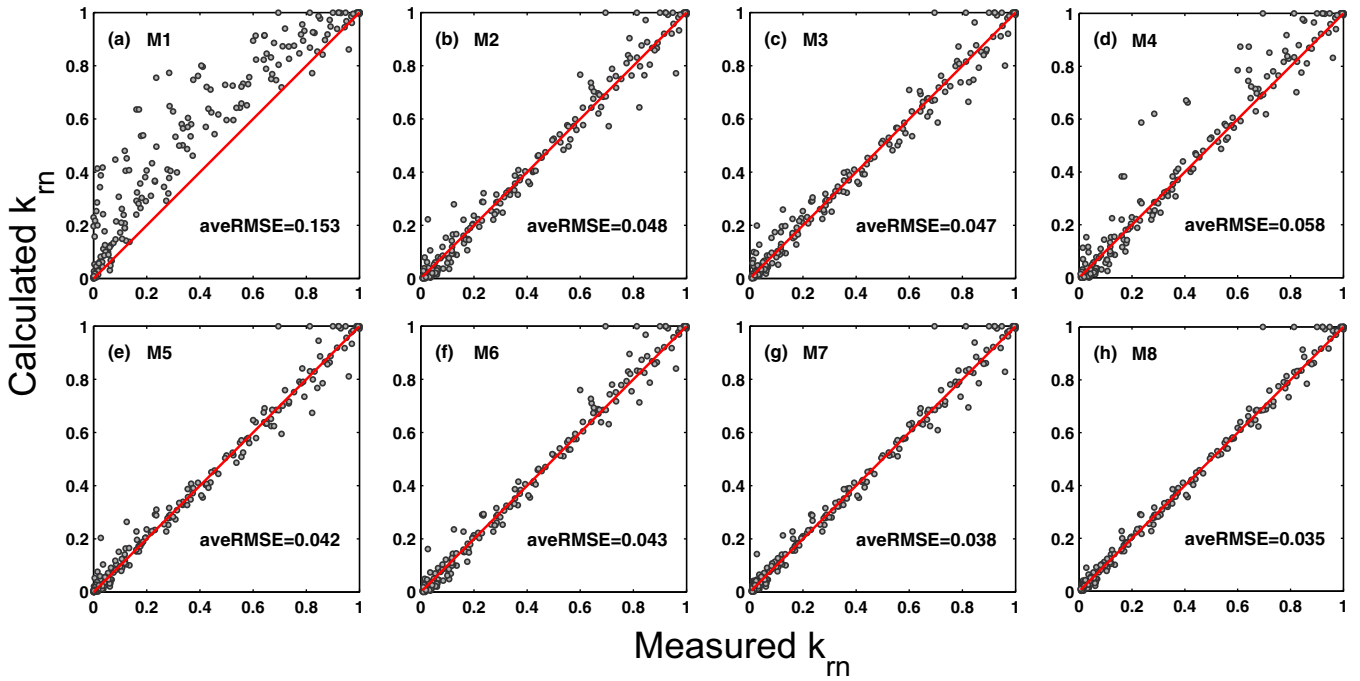

Figure 3. Scatter charts of measured versus calculated relative gas permeability for the cases (a) M1, (b) M2, (c) M3, (d) M4, (e) M5, (f) M6, (g) M7, and (h) M8 for the 17 data sets.

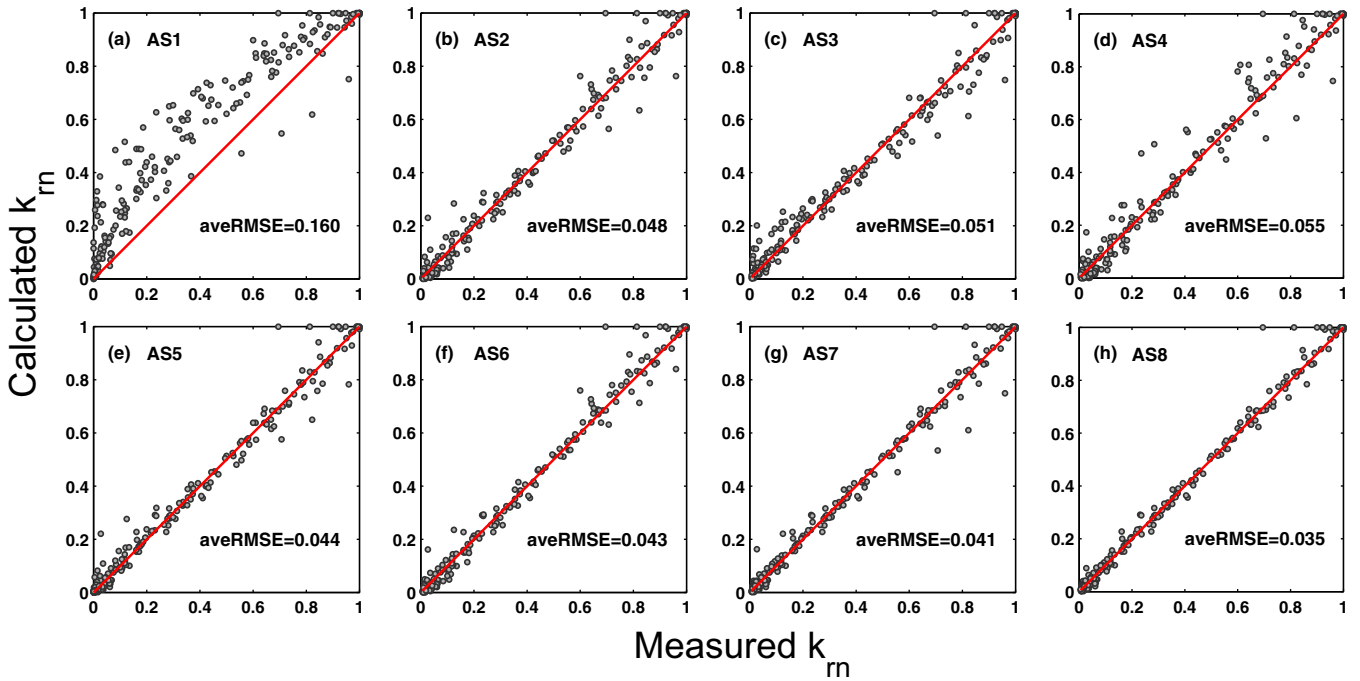

Figure 4. Scatter charts of measured versus calculated relative gas permeability for the cases (a) AS1, (b) AS2, (c) AS3, (d) AS4, (e) AS5, (f) AS6, (g) AS7, and (h) AS8 for the 17 data sets.

that the optimum α value is 2.5 for the Burdine model. The $\alpha=1/3$ in Figure 5b corresponds to the *Luckner et al.* [1989] model which has a large average RMSE value 0.178. The optimum α value for Mualem model is 2 as shown in Firgure 5b. Whereas Figure 5c illustrates that for the Alexander and Skaggs model, the optimum α value is 2.5.

As such, for the purpose of estimating k_{rn} values, the parameterizations of α, β, and η values are suggested to be equal to (2.5, 2, 1), (2, 1, 2), and (2.5, 1, 1) for the Burdine, Mualem, and Alexander and Skaggs models, respectively. The average RMSE of these three suggested models and the other six commonly used statistical models are summarized in Table 3. It can be seen from Table 3 that among the nine investigated models, the modified Burdine, modified Mualem, and modified Alexander and Skaggs permeability models have the lowest average RMSE values, which are 1.2, 2.0, and 2.2 times smaller than that of their corresponding original models, respectively. It is noticed that the improvement of prediction of k_{rn} value is more significant for the Mualem and Alexander and Skaggs models compared to the Burdine model.

A somewhat different predictive permeability model was proposed by *Assouline* [2001], who linked the η value to the coefficient of variation of *Assouline et al.* [1998] WRF. *Nasta et al.* [2013b] recently related the η value to the coefficient of variation of Kosugi WRF for the prediction of relative hydraulic conductivity.

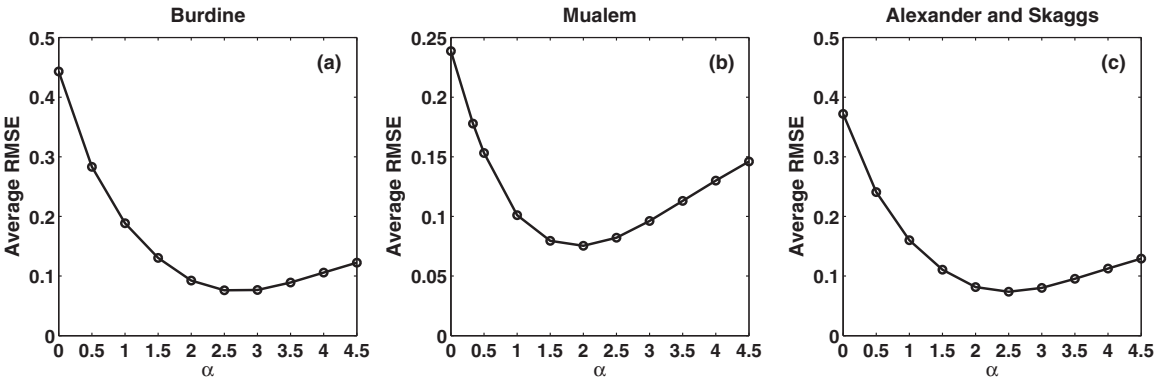

Figure 5. Variations of the average RMSE with α of the (a) Burdine, (b) Mualem, and (c) Alexander and Skaggs model.

Table 3. The Average RMSE of the Existing and Suggested Relative Gas Permeability Models

Models	α	β	η	Average RMSE
Purcell [1949]	0	2	1	0.443
Burdine [1953]	2	2	1	0.092
Mualem [1976]	0.5	1	2	0.153
Alexander and Skaggs [1986]	1	1	1	0.160
Luckner et al. [1989]	1/3	1	2	0.178
Kuang and Jiao [2011]	0.5	1	4	0.089
This study (modified Burdine)	2.5	2	1	0.076
This study (modified Mualem)	2	1	2	0.075
This study (modified AS)	2.5	1	1	0.074

However, extending *Assouline* [2001] model to calculate relative gas permeability is not quite feasible at present. This is mainly because of the scarcity of the available experimental data for simultaneously collected water retention and relative nonwetting phase permeability in the literature, compared to the vast data sets on both water retention and relative hydraulic conductivity. Therefore, a good relationship between η parameter and the coefficient of variation of *Kosugi* [1996] or *Assouline et al.* [1998] WRF on relative gas permeability cannot be determined for now. For the similar reason, any good relationship between β and σ or α and σ also cannot be found at this stage for NPRP, although *Kosugi* [1999] obtained such relationship for relative hydraulic conductivity.

4.3. Limitations of the Study

Despite the relatively comprehensive data set used and the improved models obtained in this study, there are certain limitations of our work. First, the optimum α value for relative gas permeability obtained in this study is likely to depend on the investigated data sets. One typical example in this case is that the optimum α value for relative hydraulic conductivity obtained by *Mualem* [1976] based on 45 soil samples is 0.5 while a mean value of $\alpha=-0.72$ was acquired by *Leij et al.* [1997] on the basis of another 401 soils. Therefore, it is likely that when using a different data set in future (e.g., undisturbed structured soil samples), the optimum α value for relative gas permeability will be different from the results obtained in this work. The percolation theory [*Ghanbarian-Alavijeh and Hunt*, 2012] or gas-water interfacial area based variable tortuosity-connectivity approach [*Khaleel*, 2008] could be explored in future to solve this data sets dependent optimum α value problem.

Second, the equation (5) is expected to not have good predictive capability at both very high and very low water saturation range. For the high water saturation range, equation (5) could overestimate the observed relative gas permeability, in particular, the model would still predict very small relative gas permeability while the observed NPRP is nil. This can be clearly seen from Figure 6b for Mixed sand that has the largest difference between the saturated water content and porosity, indicating the existence of a significant amount of entrapped nonwetting phase of this soil. In contrast, as Figure 6a shows, such overestimation is not quite significant for Amarillo silty clay loam which does not have large amounts of discontinuous gas (saturated water content and porosity are equal for this soil). Although the modified Mualem model can to some extent reduce the overestimation, in order to totally solve the overestimation issue at the high water saturation range, the NPRP model should take into account the discontinuous nonwetting phase as *Fischer et al.* [1997] and *Dury et al.* [1999] suggested. As a result, the NPRP model will become a function of continuous nonwetting phase saturation, rather than the total nonwetting phase saturation. However, these "analogy based" models accounting for the discontinuous nonwetting phase have the difficulty of independently and effectively determining the emergence points (i.e., the partitioning point of the total nonwetting phase into continuous and discontinuous domains) [*Dury et al.*, 1999]. On the other hand, equation (5) based on the capillary pore bundle theory ignores the liquid film flow which is known to dominate at the low water saturation range [*Tuller and Or*, 2001]. As a consequence, the NPRP model in this study would predict that the relative gas permeability is always equal to 1 when the soil water content is between 0 and θ_r, despite the possibility that the measured relative gas permeability may gradually increase to 1 in this saturation range. Therefore, as Figures 6a and 6b display, the equation (5) tends to overestimate the measured relative gas permeability at very low water saturation for both the Amarillo silty clay loam and the Mixed sand. This shortcoming can be addressed in future by incorporating the liquid film flow into equation (5) when the water content is below residual.

5. Summary and Conclusion

The relative nonwetting phase permeability is indispensable for describing the convective nonwetting phase flow in the unsaturated porous media. Combined with the Kosugi water retention function, this study

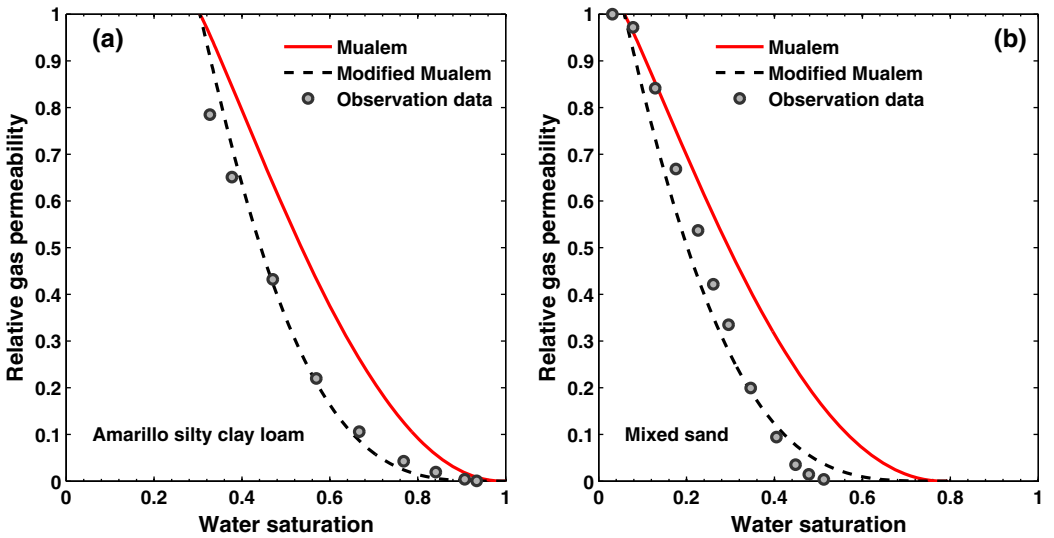

Figure 6. Comparison of measured data obtained for (a) Amarillo silty clay loam and (b) Mixed sand with predicted results using the Mualem and the Modified Mualem model.

formulated and derived a generalized expression for the nonwetting phase relative permeability, which can be used to flexibly investigate the NPRP prediction accuracy of three pore bundle models [i.e., *Burdine*, 1953; *Mualem*, 1976; *Alexander and Skaggs*, 1986]. The subsequent model and data comparison results indicate that the Burdine, Mualem, and Alexander and Skaggs models, if used in their original form, but applied to the nonwetting phase, will lead to the worst predictions of measured relative gas permeability. However, allowing one parameter (either one) among the three semiempirical parameters (α, β, and η) of the generalized NPRP model to vary can improve the fit significantly, and further increasing the degrees of freedom to two and three yields an even better fit, though with less improvement as compared to the one fitted parameter case. To this end, the optimum α value for NPRP is obtained to effectively parameterize the three investigated permeability models. Accordingly, the modified Burdine (2.5, 2, 1), the modified Mualem (2, 1, 2), and the modified Alexander and Skaggs (2.5, 1, 1) permeability model were suggested for the improved prediction of the nonwetting phase relative permeability. These three suggested permeability models have the lowest average RMSE values among all the nine investigated permeability models. In addition, the average RMSE of the modified Burdine, modified Mualem, and modified Alexander and Skaggs permeability models are 1.2, 2.0, and 2.2 times smaller than that of their corresponding original form for NPRP, respectively.

It is admitted that the optimum pore tortuosity-connectivity results for NPRP obtained in this work is likely to depend on specific data sets investigated, hence the percolation theory [*Ghanbarian-Alavijeh and Hunt*, 2012] or gas-water interfacial area based variable tortuosity-connectivity approach [*Khaleel*, 2008] should be employed in future to further investigate this parameter. In addition, the generalized expression for NPRP acquired in this study (i.e., equation (5)) does not have good predictive capability at both very high and very low water saturation ranges. To solve this issue, the future NPRP model should take into account the discontinuous nonwetting phase and liquid film flow, respectively.

Appendix A: Derivation of the Generalized NPRP Formulation With Kosugi WRF

$$\text{Due to } \int_{S_e}^{1}\frac{dS_e}{h^\beta}=\int_{0}^{1}\frac{dS_e}{h^\beta}-\int_{0}^{S_e}\frac{dS_e}{h^\beta} \tag{A1}$$

Substituting equation (3) into $\int_0^{S_e}\frac{dS_e}{h^\beta}$ leads to the integrals

$$\int_{0}^{S_e}\frac{dS_e}{h^\beta}=\frac{1}{\sqrt{2\pi}\sigma}\int_{h(S_e)}^{+\infty}\frac{1}{h^{\beta+1}}e^{-\frac{(\ln h-\ln h_m)^2}{2\sigma^2}}dh \tag{A2}$$

The change of variables $t=\ln h-\ln h_m=\ln(h/h_m)$ yields

$$\int_0^{S_e}\frac{dS_e}{h^\beta}=\frac{e^{\frac{1}{2}\beta^2\sigma^2}}{(h_m)^\beta}\frac{1}{\sqrt{2\pi}}\int_{\frac{\ln(h/h_m)}{\sigma}+\beta\sigma}^{+\infty}e^{-\frac{1}{2}\left(\frac{t}{\sigma}+\beta\sigma\right)^2}d\left(\frac{t}{\sigma}+\beta\sigma\right) \tag{A3}$$

Substituting $y=(t/\sigma+\beta\sigma)$ into equation (A3) leads to

$$\int_0^{S_e}\frac{dS_e}{h^\beta}=\frac{e^{\frac{1}{2}\beta^2\sigma^2}}{(h_m)^\beta}\frac{1}{\sqrt{2\pi}}\int_y^{+\infty}e^{-\frac{1}{2}y^2}dy \tag{A4}$$

According to the definition of complementary error function, equation (A4) becomes

$$\int_0^{S_e}\frac{dS_e}{h^\beta}=\frac{1}{(h_m)^\beta}e^{\frac{1}{2}\beta^2\sigma^2}\left\{\frac{1}{2}erfc\left[\frac{\ln(h/h_m)}{\sqrt{2}\sigma}+\frac{\beta\sigma}{\sqrt{2}}\right]\right\} \tag{A5}$$

Similarly, substituting equation (3) into $\int_0^1\frac{dS_e}{h^\beta}$ leads to the integrals

$$\int_0^1\frac{dS_e}{h^\beta}=\frac{1}{\sqrt{2\pi}\sigma}\int_0^{+\infty}\frac{1}{h^{\beta+1}}e^{-\frac{(\ln h-\ln h_m)^2}{2\sigma^2}}dh \tag{A6}$$

which becomes

$$\int_0^1\frac{dS_e}{h^\beta}=\frac{1}{(h_m)^\beta}e^{\frac{1}{2}\beta^2\sigma^2} \tag{A7}$$

Based on equation (3), one obtains

$$\frac{\ln(h/h_m)}{\sqrt{2}\sigma}=erfc^{-1}(2S_e) \tag{A8}$$

Finally, substituting equations (A1), (A5), (A7), and (A8) into equation (4) gives

$$k_{rn}=(1-S_e)^\alpha\left\{1-\frac{1}{2}erfc\left[erfc^{-1}(2S_e)+\frac{\beta\sigma}{\sqrt{2}}\right]\right\}^\eta \tag{A9}$$

which is equal to equation (5).

Acknowledgments
The authors gratefully acknowledge Jan W. Hopmans (jwhopmans@ucdavis.edu), Xingxing Kuang, and Jiu Jimmy Jiao (jjiao@hku.hk) for providing part of the data sets used in this study. Other data sets are from literature cited in the manuscript (provided in the supporting information Excel files). We are also very grateful to the anonymous reviewers for their insightful comments. This work was supported by NSF (CMG/DMS 0934837) grants.

References

Alexander, L., and R. W. Skaggs (1986), Predicting unsaturated hydraulic conductivity from the soil water characteristic, *Trans. ASAE*, *29*(1), 176–184.
Assouline, S. (2001), A model for soil relative hydraulic conductivity based on the water retention characteristic curve, *Water Resour. Res.*, *37*(2), 265–271, doi:10.1029/2000WR900254.
Assouline, S., D. Tessier, and A. Bruand (1998), A conceptual model of the soil water retention curve, *Water Resour. Res.*, *34*(2), 223–231, doi:10.1029/97WR03039.
Brooks, R. H., and A. T. Corey (1964), Hydraulic properties of porous media, *Hydrol. Pap. 3*, pp. 1–27, Colo. State Univ., Fort Collins.
Brooks, R. H., and A. T. Corey (1966), Properties of porous media affecting fluid flow, *J. Irrig. Drain. Div.*, *92*(IR2), 61–88.
Brutsaert, W. (1966), Probability laws for pore-size distributions, *Soil Sci.*, *101*(2), 85–92.
Burdine, N. T. (1953), Relative permeability calculations from pore size distribution data, *J. Pet. Technol.*, *5*(3), 71–78, doi:10.2118/225-G.
Chen, J., J. W. Hopmans, and M. E. Grismer (1999), Parameter estimation of two-fluid capillary pressure-saturation and permeability functions, *Adv. Water Resour.*, *22*(5), 479–493, doi:10.1016/S0309-1708(98)00025-6.
Collis-George, N. (1953), Relationship between air and water permeabilities in porous media, *Soil Sci.*, *76*(4), 239–250.
Corey, A. T. (1954), The interrelation between gas and oil relative permeabilities, *Prod. Mon.*, *19*(1), 38–41.
Demond, A. H., and P. V. Roberts (1993), Estimation of two-phase relative permeability relationships for organic liquid contaminants, *Water Resour. Res.*, *29*(4), 1081–1090, doi:10.1029/92WR02987.
Dury, O. (1997), Organic pollutants in unsaturated soils: Effect of butanol as a model contaminant on phase saturation and flow characteristics of a quartz sand packing, PhD thesis, Swiss Fed. Inst. of Technol., Zürich, Switzerland.
Dury, O., U. Fischer, and R. Schulin (1999), A comparison of relative nonwetting-phase permeability models, *Water Resour. Res.*, *35*(5), 1481–1493, doi:10.1029/1999WR900019.
Falta, R. W., I. Javandel, K. Pruess, and P. A. Witherspoon (1989), Density-driven flow of gas in the unsaturated zone due to the evaporation of volatile organic compounds, *Water Resour. Res.*, *25*(10), 2159–2169, doi:10.1029/WR025i010p02159.
Fatt, I., and H. Dykstra (1951), Relative permeability studies, *J. Pet. Technol.*, *3*(9), 249–255, doi:10.2118/951249-G.
Fischer, U., O. Dury, H. Flühler, and M. T. van Genuchten (1997), Modeling nonwetting-phase relative permeability accounting for a discontinuous nonwetting phase, *Soil Sci. Soc. Am. J.*, *61*(5), 1348–1354, doi:10.2136/sssaj1997.03615995006100050009x.
Gerhard, J. I., and B. H. Kueper (2003), Relative permeability characteristics necessary for simulating DNAPL infiltration, redistribution, and immobilization in saturated porous media, *Water Resour. Res.*, *39*(8), 1213, doi:10.1029/2002WR001490.
Ghanbarian-Alavijeh, B., and A. G. Hunt (2012), Comparison of the predictions of universal scaling of the saturation dependence of the air permeability with experiment, *Water Resour. Res.*, *48*, W08513, doi:10.1029/2011WR011758.

Helmig, R. (1997), *Multiphase Flow and Transport Processes in the Subsurface: A Contribution to the Modeling of Hydrosystems*, Springer, N. Y.
Hoffmann-Riem, H., M. T. van Genuchten, and H. Flühler (1999), General model for the hydraulic conductivity of unsaturated soils, in *Proceedings of the International Workshop on Characterization and Measurement of the Hydraulic Properties of Unsaturated Porous Media*, edited by M. T. van Genuchten, F. J. Leij, and L. Wu, pp. 31–42, Univ. of Calif., Riverside, Calif.
Honarpour, M. M., L. Koederitz, and A. H. Harvey (1986), *Relative Permeability of Petroleum Reservoirs*, CRC Press, Boca Raton, Fla.
Khaleel, R. (2008), Interfacial area based variable tortuosity-connectivity for unsaturated media: A comparison using Miller-Miller scaling and Arya-Paris model, *Water Resour. Res.*, *44*, W09420, doi:10.1029/2007WR006572.
Kosugi, K. (1994), Three-parameter lognormal distribution model for soil water retention, *Water Resour. Res.*, *30*(4), 891–901, doi:10.1029/93WR02931.
Kosugi, K. (1996), Lognormal distribution model for unsaturated soil hydraulic properties, *Water Resour. Res.*, *32*(9), 2697–2703, doi:10.1029/96WR01776.
Kosugi, K. (1999), General model for unsaturated hydraulic conductivity for soils with lognormal pore-size distribution, *Soil Sci. Soc. Am. J.*, *63*(2), 270–277, doi:10.2136/sssaj1999.03615995006300020003x.
Kuang, X., and J. J. Jiao (2011), A new model for predicting relative nonwetting phase permeability from soil water retention curves, *Water Resour. Res.*, *47*, W08520, doi:10.1029/2011WR010728.
Kueper, B. H., and E. O. Frind (1991), Two-phase flow in heterogeneous porous media: 1. Model development, *Water Resour. Res.*, *27*(6), 1049–1057, doi:10.1029/91WR00266.
Leij, F. J., W. B. Russell, and S. M. Lesch (1997), Closed-form expressions for water retention and conductivity data, *Ground Water*, *35*(5), 848–858, doi:10.1111/j.1745-6584.1997.tb00153.x.
Luckner, L., M. T. van Genuchten, and D. R. Nielsen (1989), A consistent set of parametric models for the two-phase flow of immiscible fluids in the subsurface, *Water Resour. Res.*, *25*(10), 2187–2193, doi:10.1029/WR025i010p02187.
Mohanty, B. P., and Z. Yang (2013), Comment on "A simulation analysis of the advective effect on evaporation using a two-phase heat and mass flow model" by Yijian Zeng, Zhongbo Su, Li Wan, and Jun Wen, *Water Resour. Res.*, *49*, 7831–7835, doi:10.1002/2013WR013489.
Mosthaf, K., K. Baber, B. Flemisch, R. Helmig, A. Leijnse, I. Rybak, and B. Wohlmuth (2011), A coupling concept for two-phase compositional porous-medium and single-phase compositional free flow, *Water Resour. Res.*, *47*, W10522, doi:10.1029/2011WR010685.
Mualem, Y. (1976), A new model for predicting the hydraulic conductivity of unsaturated porous media, *Water Resour. Res.*, *12*(3), 513–522, doi:10.1029/WR012i003p00513.
Mualem, Y., and G. Dagan (1978), Hydraulic conductivity of soils: Unified approach to the statistical models, *Soil Sci. Soc. Am. J.*, *42*(3), 392–395, doi:10.2136/sssaj1978.03615995004200030003x.
Nasta, P., N. Romano, S. Assouline, J. A. Vrugt, and J. W. Hopmans (2013a), Prediction of spatially variable unsaturated hydraulic conductivity using scaled particle-size distribution functions, *Water Resour. Res.*, *49*, 4219–4229, doi:10.1002/wrcr.20255.
Nasta, P., S. Assouline, J. B. Gates, J. W. Hopmans, and N. Romano (2013b), Prediction of unsaturated relative hydraulic conductivity from Kosugi's water retention function, *Procedia Environ. Sci.*, *19*, 609–617, doi:10.1016/j.proenv.2013.06.069.
Parker, J. C., R. J. Lenhard, and T. Kuppusamy (1987), A parametric model for constitutive properties governing multiphase flow in porous media, *Water Resour. Res.*, *23*(4), 618–624, doi:10.1029/WR023i004p00618.
Purcell, W. R. (1949), Capillary pressures: Their measurement using mercury and the calculation of permeability therefrom, *J. Pet. Technol.*, *186*, 39–48, doi:10.2118/949039-G.
Raats, P. A. C. (1992), A superclass of soils, in *Proceedings of the International Workshop on Indirect Methods for Estimating the Hydraulic Properties of Unsaturated Soils*, edited by M. Th. van Genuchten, F. J. Leij, and L. J. Lund, pp. 45–51, Univ. of Calif., Riverside, 11–13 Oct.
Seki, K. (2007), SWRC fit: A nonlinear fitting program with a water retention curve for soils having unimodal and bimodal pore structure, *Hydrol. Earth Syst. Sci. Discuss.*, *4*, 407–437, doi:10.5194/hessd-4-407-2007.
Smits, K. M., V. V. Ngo, A. Cihan, T. Sakaki, and T. H. Illangasekare (2012), An evaluation of models of bare soil evaporation formulated with different land surface boundary conditions and assumptions, *Water Resour. Res.*, *48*, W12526, doi:10.1029/2012WR012113.
Springer, D. S., H. A. Loaiciga, S. J. Cullen, and L. G. Everett (1998), Air permeability of porous materials under controlled laboratory conditions, *Ground Water*, *36*(4), 558–565, doi:10.1111/j.1745-6584.1998.tb02829.x.
Stonestrom, D. A. (1987), Co-determination and comparison of hysteresis-affected, parametric functions of unsaturated flow: Water-content dependence of matric pressure, air-trapping, and fluid permeabilities in a non-swelling soil, PhD thesis, Stanford Univ., Stanford, Calif.
Szymkiewicz, A., R. Helmig, and H. Kuhnke (2011), Two-phase flow in heterogeneous porous media with non-wetting phase trapping, *Transp. Porous Media*, *86*(1), 27–47, doi:10.1007/s11242-010-9604-x.
Touma, J., and M. Vauclin (1986), Experimental and numerical analysis of two-phase infiltration in a partially saturated soil, *Transp. Porous Media*, *1*(1), 27–55, doi:10.1007/BF01036524.
Tuli, A., and J. W. Hopmans (2004), Effect of degree of fluid saturation on transport coefficient in disturbed soils, *Eur. J. Soil Sci.*, *55*(1), 147–164, doi:10.1046/j.1365-2389.2002.00493.x-i1.
Tuli, A., J. W. Hopmans, D. E. Rolston, and P. Moldrup (2005), Comparison of air and water permeability between disturbed and undisturbed soils, *Soil Sci. Soc. Am. J.*, *69*(5), 1361–1371, doi:10.2136/sssaj2004.0332.
Tuller, M., and D. Or (2001), Hydraulic conductivity of variably saturated porous media: Film and corner flow in angular pore space, *Water Resour. Res.*, *37*(5), 1257–1276, doi:10.1029/2000WR900328.
van Genuchten, M. T. (1980), A closed-form equation for predicting the hydraulic conductivity of unsaturated soils, *Soil Sci. Soc. Am. J.*, *44*(5), 892–898, doi:10.2136/sssaj1980.03615995004400050002x.